

This discussion paper is/has been under review for the journal Atmospheric Chemistry and Physics (ACP). Please refer to the corresponding final paper in ACP if available.

**H<sub>2</sub>O and O<sub>3</sub>  
anomalies during  
major SSW in  
January 2010**

D. Scheiben et al.

# Middle atmospheric water vapor and ozone anomalies during the 2010 major sudden stratospheric warming

D. Scheiben<sup>1</sup>, C. Straub<sup>1</sup>, K. Hocke<sup>1,2</sup>, P. Forkman<sup>3</sup>, and N. Kämpfer<sup>1</sup>

<sup>1</sup>Institute of Applied Physics, University of Bern, Bern, Switzerland

<sup>2</sup>Oeschger Center for Climate Research, University of Bern, Bern, Switzerland

<sup>3</sup>Department of Earth and Space Sciences, Chalmers University of Technology, Gothenburg, Sweden

Received: 7 October 2011 – Accepted: 29 November 2011 – Published: 8 December 2011

Correspondence to: D. Scheiben (dominik.scheiben@iap.unibe.ch)

Published by Copernicus Publications on behalf of the European Geosciences Union.

Title Page

Abstract

Introduction

Conclusions

References

Tables

Figures

⏪

⏩

◀

▶

Back

Close

Full Screen / Esc

Printer-friendly Version

Interactive Discussion

## Abstract

A major sudden stratospheric warming (SSW) occurred in the Northern Hemisphere in January 2010. The warming started on 26 January 2010, was most pronounced by the end of January and was accompanied by a polar vortex shift towards Europe.

5 After the warming, the polar vortex split into two weaker vortices. The zonal mean temperature in the polar upper stratosphere (35–45 km) increased by approximately 25 K in a few days, while there was a decrease in temperature in the lower stratosphere and mesosphere. Local temperature maxima were around 325 K in the upper stratosphere and minima around 175 and 155 K in the lower stratosphere and mesosphere, respectively. In this study, we present middle atmospheric water vapor and ozone  
10 measurements obtained by a meridional chain of European ground-based microwave radiometers in Bern (47° N), Onsala (57° N) and Sodankylä (67° N). The instruments in Bern and Onsala are part of the Network for the Detection of Atmospheric Composition Change (NDACC). Effects of the SSW were observed at all three locations and we perform a combined analysis in order to reveal transport processes in the middle  
15 atmosphere above Europe during the SSW event. Further we investigate the chemical and dynamical influences of the SSW event. We find that the anomalies during the warming in water vapor and ozone were different for each location. A few days before the beginning of the major SSW, we observed a decrease in mesospheric water vapor above Bern, which we attribute to movement of the mesospheric polar vortex towards Central Europe. The most prominent H<sub>2</sub>O anomaly observed in Bern was an increase in stratospheric water vapor during the warming. In Onsala and Sodankylä, mesospheric water vapor increased within a few days during the warming and slowly decreased afterwards. Upper stratospheric ozone decreased during the warming over  
20 Bern by approximately 30 % and by approximately 20 % over Onsala. Over Sodankylä, a decrease in ozone below 30 km altitude was observed. This decrease is assumed to be caused by heterogeneous chemistry on polar stratospheric clouds. After the SSW, stratospheric ozone increased to higher levels than before at all three locations. The  
25

### H<sub>2</sub>O and O<sub>3</sub> anomalies during major SSW in January 2010

D. Scheiben et al.

Title Page

Abstract

Introduction

Conclusions

References

Tables

Figures



Back

Close

Full Screen / Esc

Printer-friendly Version

Interactive Discussion



---

## H<sub>2</sub>O and O<sub>3</sub> anomalies during major SSW in January 2010

D. Scheiben et al.

---

Title Page

Abstract

Introduction

Conclusions

References

Tables

Figures

⏪

⏩

◀

▶

Back

Close

Full Screen / Esc

Printer-friendly Version

Interactive Discussion



observed anomalies are explained by a trajectory analysis with reanalysis data from the European Center for Medium-Range Weather Forecasts (ECMWF). Most of the observed anomalies in water vapor and ozone during the warming are attributed to the location of the polar vortex, depending on whether a measurement site was inside or outside the polar vortex. The observed increase in mesospheric water vapor at high latitudes is explained by advection of relatively moist air from lower latitudes, whereas the observed increase in stratospheric water vapor at midlatitudes is explained by advection from high latitudes, i.e. from the moist stratospheric polar vortex.

### 1 Introduction

The lack of solar radiation at the winter pole forms a large low pressure system over the polar region. This low pressure system leads to strong eastward winds around the North Pole, forming the typical winter time polar vortex. The edge of the vortex is a mixing barrier such that the air inside the vortex is considerably colder and has a different chemical composition than outside (e.g., Schoeberl et al., 1992; Manney et al., 1994). The polar vortex exists from the troposphere up to the mesosphere, but is strongest in the stratosphere. In the mesosphere, the vortex area is larger than in the middle stratosphere, i.e. the polar night jet is located at lower latitudes than in the stratosphere (see e.g. Harvey et al., 2009, and references therein). Inside the polar vortex, the air is descending from the mesosphere to the stratosphere, which was modeled e.g. by Rosenfield et al. (1994) or observed e.g. by Allen et al. (2000). During a quiet winter, the vortex is persistent throughout the whole winter and disappears in the beginning of spring. During some winters however, the polar vortex is seriously disturbed or destroyed by sudden stratospheric warmings (SSW), which were discovered by Sherhag (1952). A SSW is a sudden increase in the stratospheric temperature, often accompanied by a reversal of the zonal wind. The occurrence frequency of SSWs between 1958 and 2001 is approximately  $0.6 \text{ yr}^{-1}$ , according to Table 1 in Charlton and Polvani (2007).

## H<sub>2</sub>O and O<sub>3</sub> anomalies during major SSW in January 2010

D. Scheiben et al.

Title Page

Abstract

Introduction

Conclusions

References

Tables

Figures



Back

Close

Full Screen / Esc

Printer-friendly Version

Interactive Discussion



The occurrence of a SSW was found to be due to the interaction of the zonal mean flow (eastward) with westward propagating planetary waves (Matsuno, 1971). These planetary waves act to decelerate the zonal mean flow which leads to distortion and/or breakdown of the polar night jet. This wave-mean flow interaction triggers a displacement, disruption and/or splitting of the polar vortex (Charlton and Polvani, 2007). The strongest major SSW observed up to date occurred in winter 2008/2009 at the end of January 2009 (e.g. Manney et al., 2009; Labitzke and Kunze, 2009). A major warming in the stratosphere is always accompanied by a cooling in the mesosphere. The mesospheric cooling usually starts a few days earlier than the stratospheric warming (Schoeberl, 1978). This coupling between two or more atmospheric layers during a SSW was the focus of many recent studies. Manney et al. (2008a,b) and Orsolini et al. (2010) showed that after an SSW, the stratopause often reforms at approximately 75 km altitude which is the typical altitude of the upper mesosphere. Martius et al. (2009) showed that atmospheric blocking situations in the troposphere could be a trigger of the sudden warmings in the stratosphere. Goncharenko et al. (2010) showed that SSWs also have an impact on the lower thermosphere and ionosphere in the equatorial region.

Flury et al. (2009) showed that the major SSW during the winter 2007/2008 led to a decrease in lower stratospheric ozone. This ozone decrease was triggered by the formation of polar stratospheric clouds (PSC) due to temperatures below 195 K in the lower stratosphere. At the same time, ozone decreased in the relatively warm upper stratosphere due to the temperature dependence of the NO<sub>x</sub> cycle. The geographical extension of an SSW can range down to the subtropics, as was shown by De Wachter et al. (2011). They also studied the SSW of 2008 and observed a decrease in mesospheric water vapor over Seoul, South Korea, which was attributed to advection of dry polar mesospheric air to the subtropics. Lahoz et al. (2011) used assimilated middle atmospheric water vapor observations as a tracer to study the 2009 SSW and calculated descent rates in the polar vortex based on water vapor assimilations. Hartogh et al. (2011) explained the observed weak ozone maximum in late winter in the midlatitudinal

mesopause region by the activity of SSWs, which reduced ozone in this altitude region in January and February.

In winter 2009/2010, two SSWs occurred in the Northern Hemisphere, a minor warming in the beginning of December 2009 and a major warming at the end of January 2010. The terms minor and major warming refer to the characterization of SSWs according to the Commission for Atmospheric Sciences of the World Meteorological Organization (WMO), which is based on the work of McInturff (1978). Thanks to new remote sensing instruments and advances in modeling of the whole atmosphere system in recent years, the impact of SSWs on atmospheric composition and circulation can now be studied in more detail.

We focus on exchange processes between polar and subtropical air in the middle atmosphere during a SSW and use measurements from ground-based instruments within NDACC from midlatitudes up to high latitudes. There is one midlatitudinal location, Bern, Switzerland (46.9° N/7.45° E) and two Scandinavian sites, Onsala, Sweden (57.4° N/12.0° E) and Sodankylä, Finland (67.4° N/26.6° E). In this study, we present observations of middle atmospheric water vapor and ozone for these locations during the major SSW from January 2010. Satellite data of water vapor and ozone from the Microwave Limb Sounder on the Aura satellite (Aura MLS) is used to fill in gaps in the data from the three locations. This is the first study that uses a mini-network of three locations with ground-based instruments to study the effects of a SSW on middle atmospheric water vapor and ozone.

The next section, Sect. 2, describes the data sources and gives references for further details of the instruments and models used. The first part of Sect. 3 describes the January 2010 SSW from a global view, the second part from a local view at our measurement locations. The fourth and fifth sections show the observed water vapor and ozone anomalies and give explanations by means of trajectory analyses and determination of the location of the polar vortex. Section 6 concludes the presented material and explanations.

**H<sub>2</sub>O and O<sub>3</sub> anomalies during major SSW in January 2010**

D. Scheiben et al.

Title Page

Abstract

Introduction

Conclusions

References

Tables

Figures



Back

Close

Full Screen / Esc

Printer-friendly Version

Interactive Discussion



## 2 Data sources

The observational data presented in this study are obtained by ground-based and spaceborne microwave radiometers. Microwave radiometers are passive instruments measuring a spectrum around a rotational emission line of the molecule of interest, in our case 22.235 GHz for water vapor and 142 GHz for ozone. The microwave emission of these molecules is a pressure broadened spectrum. Pressure broadening allows retrieving a vertical profile of the molecule of interest for example by the Optimal Estimation Method (OEM) (see for example Rodgers, 2000). The upper limit of the retrieval is mainly determined by the resolution of the spectrometer, the lower limit by the total measured bandwidth and the baseline of the spectrum.

For Bern, Switzerland, we use water vapor profiles from the Middle Atmospheric WATER vapor RADIometer (MIAWARA) (Deuber et al., 2005). Its valid vertical range is between 10 and 0.02 hPa, the temporal resolution depends on tropospheric opacity and is a few hours during wintertime. MIAWARA was validated against the satellite instrument MLS on the Aura satellite and has a bias of less than 10 % in the stratosphere and mesosphere (Haeferle et al., 2009). Ozone profiles for Bern are measured by the GROUND-based Millimeter-wave Ozone Spectrometer (GROMOS), which has a valid vertical range between 60 and 0.1 hPa with a temporal resolution of a few minutes (Calisesi et al., 2001). In the present study, 2-hourly ozone profiles are used. Both instruments, MIAWARA and GROMOS, are part of the Network for the Detection of Atmospheric Composition Change (NDACC). The vertical resolution of both instruments is approximately 10 km in the stratosphere and the mesosphere. The water vapor data presented for Onsala, Sweden, is also obtained by a ground-based microwave radiometer with similar characteristics as MIAWARA (Forkman et al., 2003) and is also part of NDACC. There have been difficulties in the operation of this radiometer in winter 2009/2010 resulting in data gaps, which are complemented by data from Aura MLS. Ozone data for Onsala is also from Aura MLS. The water vapor data over Sodankylä is obtained from the compact radiometer MIAWARA-C (Straub et al., 2010). This instru-

### H<sub>2</sub>O and O<sub>3</sub> anomalies during major SSW in January 2010

D. Scheiben et al.

Title Page

Abstract

Introduction

Conclusions

References

Tables

Figures



Back

Close

Full Screen / Esc

Printer-friendly Version

Interactive Discussion



ment, which has been specifically designed for the use in measurement campaigns, was operated from Sodankylä in the frame of the Lapland Atmosphere-Biosphere Facility (LAPBIAT) campaign. MIAWARA-C's daily profiles cover an altitude range between 10 and 0.02 hPa with a vertical resolution of approximately 12 km.

The Microwave Limb Sounder on NASA's Aura satellite (Aura MLS) is a passive limb sounder for the retrieval of various trace species, geopotential height and temperature data (Waters et al., 2006). The vertical resolution of Aura MLS ranges from 3 to 6 km for water vapor in the middle atmosphere (Lambert et al., 2007). The Aura MLS retrieval version used for this study is 3.3 and data is only considered within the valid vertical range and if quality thresholds are met as given in Table 1.1.1 of the version 3.3 data quality document (<http://mls.jpl.nasa.gov/data/datadocs.php>). Satellite profile selection for a given location is within the given latitude  $\pm 400$  km and the given longitude  $\pm 800$  km.

Meteorological reanalysis data from the European Center for Medium-Range Weather Forecasts (ECMWF) is used for descriptions of the polar vortex and tropospheric temperature. Trajectory calculations are performed using the Lagrangian Trajectory Tool LAGRANTO, developed at the ETH Zurich (Wernli and Davies, 1997). We use the 3-D wind fields from the ECMWF operational data set for trajectory calculations and the ECMWF ERA-INTERIM Re-Analysis (Dee et al., 2011) for all other purposes. The operational and the ERA-INTERIM data set have their upper model limit at 0.01 hPa (approximately 80 km) and 0.1 hPa (approximately 64 km), respectively.

To summarize the data sources, Table 1 lists all instruments and models used for the three different locations.

**H<sub>2</sub>O and O<sub>3</sub> anomalies during major SSW in January 2010**

D. Scheiben et al.

Title Page

Abstract

Introduction

Conclusions

References

Tables

Figures



Back

Close

Full Screen / Esc

Printer-friendly Version

Interactive Discussion



### 3 The SSW in January 2010

#### 3.1 Water vapor and ozone in the polar vortex

To support the readers' understanding of the middle atmospheric composition in water vapor and ozone, Fig. 1 shows typical winter time water vapor, ozone and temperature profiles inside and outside of the polar vortex, obtained from Aura MLS measurements during winter 2009/2010 before the major SSW. The location of the polar vortex is determined qualitatively by isentropic potential vorticity (PV) maps in the stratosphere (relatively high PV corresponds to the polar vortex) and by the area enclosed by the polar night jet in the mesosphere, based on absolute wind speeds. The temperature minima and maxima in the lower stratosphere and at the stratopause, respectively, are lower in temperature and higher in altitude inside the vortex than outside. The stratopause, i.e. the temperature maximum in the middle atmosphere, is found at approximately 58 km altitude inside and at 46 km outside the vortex. The reason for the high polar stratopause is the subsidence of air inside the vortex and corresponding adiabatic heating. Inside the polar vortex, the volume mixing ratio of water vapor has a maximum of approximately 7 parts per million (ppm) in the stratosphere at 32 km and then decreases with height by approximately 1 ppm per 10 km. Outside of the vortex, the stratospheric water vapor mixing ratio is lower than inside the vortex. Water vapor outside of the vortex has a maximum at the stratopause and the lower mesosphere between 50 and 60 km of 7–8 ppm and then decreases with height by approximately 2.5 ppm per 10 km. The increase of water vapor with height from the tropopause to the stratopause arises from methane oxidation, the decrease above the stratopause is due to photodissociation of water vapor (Brasseur and Solomon, 2005). The Brewer-Dobson circulation (Brewer, 1949) transports middle atmospheric air from low latitudes to high latitudes, where the subsidence of the air inside the polar vortex leads to the observed water vapor maximum at altitudes approximately 20 km below the maximum outside of the vortex. The stratospheric ozone maximum outside of the vortex has mixing ratios of up to 8 ppm, which is higher than inside the vortex where the maximum

32398

## H<sub>2</sub>O and O<sub>3</sub> anomalies during major SSW in January 2010

D. Scheiben et al.

Title Page

Abstract

Introduction

Conclusions

References

Tables

Figures

⏪

⏩

◀

▶

Back

Close

Full Screen / Esc

Printer-friendly Version

Interactive Discussion



mixing ratios are approximately 5 ppm. The low ozone content in the polar vortex is due to the mixing barrier at the edge of the vortex which diminishes the transport from the low latitudes, where ozone is produced, to the inside of the vortex. Due to the different mixing ratios inside and outside of the vortex, water vapor and ozone can be used as tracers for studying middle atmospheric dynamics and transport processes in the midlatitudes and polar region, in particular in the region of the vortex edge.

### 3.2 The global view

The upper panel in Fig. 2 shows the zonal mean temperature at 10 hPa during winter 2009/2010 against latitude and time. In December and January a strong temperature gradient from 45° N towards the North Pole due to the polar vortex is present, which was disturbed twice at the beginning of December and at the end of January, when the two SSWs occurred. The first anomaly in the temperature gradient was a minor SSW, as the temperature gradient remained negative towards the pole and the zonal mean zonal wind did not reverse (lower panel in Fig. 2). The second anomaly at the end of January was a major SSW fulfilling the major SSW criteria from the WMO: The zonal mean temperature gradient at 10 hPa was positive from 60° N towards the pole and the zonal mean zonal wind reversed from westerly to easterly at latitudes poleward of 60° N. The strong negative temperature gradient from before the major SSW did not recover after the major SSW, i.e. the polar vortex did not re-form to its original strength.

Figure 3 shows ECMWF PV on the 850 K isentropic surface (at approximately 10 hPa) before (16 and 21 January), during (26 and 31 January) and after the major SSW (5 and 10 February). The white circles indicate the positions of the microwave radiometers. Before the warming, the stratospheric vortex was already slightly shifted towards Europe and Asia due to the Aleutian High. In the beginning of the warming, the vortex was displaced and then in the course of the warming split into a larger vortex moving westward and a smaller vortex moving eastward. Hence, in this particular case, a clear distinction between a displacement and a splitting event is not possible. Figure 3 also shows that each measurement location was occasionally inside and outside

## H<sub>2</sub>O and O<sub>3</sub> anomalies during major SSW in January 2010

D. Scheiben et al.

Title Page

Abstract

Introduction

Conclusions

References

Tables

Figures

⏪

⏩

◀

▶

Back

Close

Full Screen / Esc

Printer-friendly Version

Interactive Discussion



of the vortex and that the vortex even extended to the midlatitudes. Thus we analyze the difference of inside-vortex air and outside-vortex air in chemical composition, temperature and vertical structure of trace gas profiles such as water vapor.

### 3.3 The local view

5 The increase in upper stratospheric temperature during the minor and the major SSW was observed in the time series of temperature in Fig. 4 at Bern (47° N, upper panel), Onsala (57° N, middle panel) and Sodankylä (67° N, lower panel). During the SSW, the stratopause descended at all locations, most pronounced at higher latitudes. For all locations, the temperature at the stratopause decreased after the warming. Coinciding  
10 with the warming in the upper stratosphere there was a cooling of the mesosphere during the minor and the major warming. During the major SSW, a cooling in the lower stratosphere over Bern was also observed which started a few days earlier than the SSW. The upper stratospheric warming and lower stratospheric cooling over Bern will be examined here by a trajectory analysis.

15 The isentropes are descending at the height of the warming and ascending where cooling takes place, indicating adiabatic warming and cooling, respectively. To illustrate this link between the vertical movement of middle atmospheric air and the observed temperature anomalies, we calculated backward trajectories over Bern with LAGRANTO based on ECMWF wind fields. We calculated 72 h backward trajectories  
20 every 6 h from three weeks before to two weeks after the observed SSW over Bern. At every time step, the trajectories started from 5 different pressure levels (30, 10, 3, 1 and 0.3 hPa). The result is shown in Fig. 5. Since we are interested in the vertical movement of air, only pressure vs. time for each individual trajectory is shown. Clearly visible is the subsidence of air in the region of the warming (3 hPa) from 25 January  
25 to 1 February: Almost every air parcel originated from higher altitudes and the subsidence led to adiabatic heating. The situation was opposite for the region of the cooling at 30 hPa, where ascending air led to the observed cooling between 24 January and 4 February. The rise of the air parcels in the cooling region is less pronounced than the

## H<sub>2</sub>O and O<sub>3</sub> anomalies during major SSW in January 2010

D. Scheiben et al.

Title Page

Abstract

Introduction

Conclusions

References

Tables

Figures

⏪

⏩

◀

▶

Back

Close

Full Screen / Esc

Printer-friendly Version

Interactive Discussion



descent of air in the warming region. This lower stratospheric cooling over Bern was also observed during a major SSW two years earlier by Flury et al. (2009).

The observed deceleration of zonal wind at 10 hPa during the SSW (Fig. 2) is associated with downward and poleward air motion according to conservation of angular momentum. The observed adiabatic warming (descent of air) is thus consistent with the decrease in zonal wind. Accordingly, the zonal wind in the altitude region of the stratospheric cooling, i.e. between approximately 100 and 30 hPa, has increased during the SSW (not shown here), which must lead to upward and equatorward air motion. This is again consistent with the observed adiabatic cooling.

## 4 Water vapor and ozone anomalies

### 4.1 Water vapor and ozone over Bern

Figure 6 shows the time series of water vapor and ozone over Bern measured by the ground based instruments MIAWARA and GROMOS, respectively. During the time of the major SSW, MIAWARA observed an increase of the water vapor mixing ratio by approximately 20 % in the stratosphere between 20 and 7 hPa correlating with an increase in PV, as seen from the variations of the PV contour lines in the upper panel of Fig. 6. The correlation between stratospheric water vapor and PV was also stated by Schoeberl et al. (1992). PV is a good indicator for the latitudinal and vertical origin of an air parcel, as it is a good tracer. Stratospheric water vapor increases with height and latitude, hence the observed water vapor anomaly is linked with vertical and/or latitudinal advection. This stratospheric water vapor enhancement during a major SSW is consistent with previous studies (see e.g. Flury et al., 2009). After the major SSW, PV decreased and MIAWARA observed very low mixing ratios of stratospheric water vapor at this altitude. During the minor warming, an increase in stratospheric water vapor was not observed. Stratospheric ozone concentrations decreased during the minor warming by approximately 20 % from 6 to 5 ppm and during the major warming

## H<sub>2</sub>O and O<sub>3</sub> anomalies during major SSW in January 2010

D. Scheiben et al.

Title Page

Abstract

Introduction

Conclusions

References

Tables

Figures

⏪

⏩

◀

▶

Back

Close

Full Screen / Esc

Printer-friendly Version

Interactive Discussion





more variable than over Bern and over Sodankylä, but the anomalies caused by the two SSWs are still evident.

Stratospheric ozone decreased slightly during the minor SSW and strongly during the major SSW. The decrease in stratospheric ozone correlates with an increase in PV, indicating origin of the air from the polar vortex. The upper stratospheric ozone mixing ratio at Onsala was approximately 4 ppm during the SSW which is comparable to the stratospheric mixing ratios at Sodankylä (lower panel of Fig. 8), which is 10 degrees further north. After the major SSW, upper stratospheric ozone, i.e. between 10 and 1 hPa increased to higher values than before the warming. However, in the lower stratosphere between 50 and 10 hPa, ozone concentrations were very low until 20 February. The low ozone concentrations are possibly due to polar stratospheric clouds (PSCs), i.e. PSCs activate catalytic ozone destruction cycles by heterogeneous reactions of chlorine reservoir compounds on the surface of the PSC particles. Such PSCs were observed over Northern Europe during the time of the major SSW.

### 4.3 Water vapor and ozone over Sodankylä

The two SSWs during winter 2009/2010 had a strong impact on mesospheric water vapor over Sodankylä (Fig. 8). During the minor and the major warming, mesospheric water vapor at 0.1 hPa increased by approximately 50 % from 5 to 7.5 ppm. The vortex shift and disruption during the major SSW led to mixing of dry polar mesospheric air with midlatitudinal, more humid air. The rapid water vapor increase was followed by a slow decrease which prolonged until mid-March. The subsidence of polar mesospheric air during winter is seen by the slope of the isolines of water vapor and is indicated by the magenta line in Fig. 8. The increase in mesospheric water vapor at middle and high latitudes during a SSW is consistent with previous studies, e.g. Seele and Hartogh (2000) or Flury et al. (2009). The stratospheric ozone concentration over Sodankylä decreased steadily during winter until the end of January. Only minor disturbances were observed during the minor warming. However, the major SSW led to a strong ozone increase between 10 and 1 hPa of more than 50 % over Sodankylä. The

## H<sub>2</sub>O and O<sub>3</sub> anomalies during major SSW in January 2010

D. Scheiben et al.

Title Page

Abstract

Introduction

Conclusions

References

Tables

Figures

⏪

⏩

◀

▶

Back

Close

Full Screen / Esc

Printer-friendly Version

Interactive Discussion



increase was caused by mixing of midlatitudinal, ozone rich air into the polar region. The upper stratospheric ozone concentration then remained on high levels for the rest of the winter, which is due to the breakdown of the polar vortex and the corresponding mixing with air masses from lower latitudes. In the lower stratosphere, ozone concentrations remained very low until 20 February due to the same effect as over Onsala, i.e. due to catalytic ozone destruction caused by PSCs.

## 5 Trajectories from Bern, Onsala and Sodankylä

To support our interpretation of the observed anomalies, we calculated 96 h-backward trajectories at selected times and altitudes from the three locations. The backward trajectories reveal the geographic origin of the measured air parcels. Water vapor is a good tracer in the middle atmosphere due to its long lifetime and is assumed to remain constant along the trajectories. The starting time and altitude of the backward trajectories is marked in the water vapor and ozone time series (Figs. 6–8) with black crosses.

The two plots in Fig. 9 show the 96 h-backward trajectories started at 0.1 hPa superposed on polar maps of absolute wind speed in the mesosphere on the 3400 K isentropic surface (corresponds to approximately 64 km altitude) at the end of the trajectories. Since the distribution of mesospheric PV is difficult to interpret and mesospheric PV is in most cases not “vortex-centered” (Harvey et al., 2009), we plotted absolute wind speed to get an idea of the location of the polar night jet which encloses the mesospheric polar vortex. In the stratosphere, we plotted isentropic PV for the visualization of the polar vortex (Figs. 3 and 10). Please note that the wind direction in the circumpolar mesospheric jet during the SSW (right panel in Fig. 9) is westward, corresponding to the wind reversal. The trajectories before the major SSW indicate a counter clockwise (eastward) circulation, which is typical for a vortex-like circulation in the Northern Hemisphere. In addition to this circulation, the mesospheric air is descending (not shown here). This subsidence inside the mesospheric vortex-like circulation leads to

## H<sub>2</sub>O and O<sub>3</sub> anomalies during major SSW in January 2010

D. Scheiben et al.

Title Page

Abstract

Introduction

Conclusions

References

Tables

Figures



Back

Close

Full Screen / Esc

Printer-friendly Version

Interactive Discussion



## H<sub>2</sub>O and O<sub>3</sub> anomalies during major SSW in January 2010

D. Scheiben et al.

Title Page

Abstract

Introduction

Conclusions

References

Tables

Figures

⏪

⏩

◀

▶

Back

Close

Full Screen / Esc

Printer-friendly Version

Interactive Discussion

the observed low mesospheric water vapor values at Onsala and Sodankylä during the undisturbed winter situation, e.g. before the minor and major SSW. The mesosphere above Sodankylä is usually in the regime of the polar vortex, but the mesosphere above Onsala and Bern lies in the transition zone between the polar vortex and the midlatitudes and subtropics, respectively. This is visible in the observed water vapor above 5 Onsala and Bern at 0.1 hPa, which is more variable than mesospheric water vapor over Sodankylä, and the mixing ratio depends mostly on the location and extent of the polar vortex. Just before the major SSW, MIAWARA measured low concentrations of water vapor above Bern at 0.1 hPa and the backward trajectory shows that this air originated 10 from the edge of the vortex, which can also be seen by the location of the polar night jet. Hence, the low mesospheric water vapor content (of polar vortex origin) observed over Bern a few days before the actual beginning of the SSW was a first signature of the major SSW, while in the stratosphere, the first signatures in water vapor and ozone were observed a few days later, coinciding with the beginning of the SSW. Coinciding 15 with the mesospheric water vapor decrease before the warming, temperatures above Bern increased (as seen in Fig. 4). This is consistent with the shift of the mesospheric vortex (which has a generally a warmer mesosphere) towards Bern. At all three measurement locations, the mesospheric circulation changed abruptly at the beginning of the major SSW. The trajectories on the right plot of Fig. 9 originate from low latitudes and rotate clockwise towards the measurement locations. This explains the relatively 20 high water vapor mixing ratios above the two polar stations during the SSW due to the breakdown of the vortex. Over Bern, the mesospheric water vapor mixing ratios increased again to typical “outside-vortex” values.

The plots in Fig. 10 are similar to the plots in Fig. 9 but for the stratosphere at 1000 K 25 (corresponds to approximately 36 km altitude) and for the times during (29 January 2010) and after the major SSW (6 February 2010). The trajectories are now superposed on isentropic PV instead of absolute wind speed, since PV is usually “vortex-centered” in the stratosphere and can thus be used to determine the location of the polar vortex. All stratospheric trajectories during the major SSW (left plot) show a clear

## H<sub>2</sub>O and O<sub>3</sub> anomalies during major SSW in January 2010

D. Scheiben et al.

Title Page

Abstract

Introduction

Conclusions

References

Tables

Figures

⏪

⏩

◀

▶

Back

Close

Full Screen / Esc

Printer-friendly Version

Interactive Discussion



vortex-like, counter clockwise circulation. The strong shift of the polar vortex towards Europe in the course of the SSW explains the very low ozone values in the stratosphere above Bern, because Bern usually lies outside the polar vortex, i.e. has a relatively high stratospheric ozone mixing ratio. The vortex shift also explains the high stratospheric water vapor mixing ratio above Bern from approximately 20 to 6 hPa during the SSW which anti-correlates with the ozone mixing ratio. After the vortex shifted towards west away from Bern, the air above Bern at 6 hPa was coming from southeast, as shown in Fig. 10 in the right plot. The stratospheric observations of the low water vapor mixing ratio and exceptionally high ozone mixing ratio are thus consistent with the low-latitudinal origin of the observed air mass. The position of the polar vortex also explains the low stratospheric ozone values above Onsala during the major SSW, because Onsala was situated near the center of the vortex during the SSW. As Sodankylä was located within the vortex throughout most of the winter, a vortex shift acted mainly to increase stratospheric ozone over Sodankylä by advection of ozone-rich air from outside the vortex. After the major SSW, the stratospheric ozone mixing ratio increased over Onsala and Sodankylä, but not as strong as over Bern. The three trajectories after the SSW give a reason for the difference in the ozone anomalies: The stratosphere above Bern was at the edge of a high pressure system (clockwise rotation) centered over Eastern Europe which brought ozone rich air from the subtropics towards Bern. However, the two high latitude stations were still at the eastern edge of the polar vortex, which was at that time centered over Greenland and brought low-latitudinal air by the cyclonic rotation towards Onsala and Sodankylä.

## 6 Conclusions

This study combined observations of several ground-based radiometers located across Europe to obtain a regional view on the changes in middle atmospheric water vapor and ozone above Europe in the course of the major SSW of January 2010. The observations were obtained by a mini-network of ground based microwave radiometers

---

## H<sub>2</sub>O and O<sub>3</sub> anomalies during major SSW in January 2010

D. Scheiben et al.

---

[Title Page](#)[Abstract](#)[Introduction](#)[Conclusions](#)[References](#)[Tables](#)[Figures](#)[Back](#)[Close](#)[Full Screen / Esc](#)[Printer-friendly Version](#)[Interactive Discussion](#)

from NDACC, located in Bern, Onsala and Sodankylä, and from Aura MLS. The warming of the upper stratosphere and anomalies in water vapor and ozone were observed from all three locations. Over Bern, increased stratospheric water vapor and low ozone concentrations were observed during the SSW which is attributed to a combination of downwelling air masses and a shift of the polar vortex to Bern by the SSW event. Thus ozone-poor air masses were advected towards Bern during the SSW and ozone was further depleted since the warming accelerated the catalytic NO<sub>x</sub> cycle. A first signal of the SSW, a few days before the actual start of the SSW, was observed over Bern in terms of low mesospheric water vapor mixing ratios, attributed to the shift of the mesospheric vortex towards Central Europe. At the two high latitude stations Onsala and Sodankylä, the water vapor anomalies were most prominent in the mesosphere where water vapor increased abruptly with the beginning of the SSW. This increase was attributed to the breakdown of the mesospheric vortex and mixing of water vapor rich air from the midlatitudes. Decreases of upper stratospheric ozone during the SSW were also seen over Bern and Onsala but not over Sodankylä. However, low ozone concentrations were measured in the lower polar stratosphere, i.e. between 50 and 10 hPa, which are assumed to be linked to ozone depletion driven by heterogeneous reactions on PSCs.

The changes in mesospheric dynamics due to the SSW give evidence to a strong coupling between the stratosphere and the mesosphere. Trajectories, commonly used in the troposphere and lower stratosphere, are found to be a good tool to study middle atmospheric dynamics, and proved to be especially useful also in the mesosphere. The mesospheric as well as the stratospheric trajectories are consistent with our ground-based observations of water vapor and ozone and helped understanding the processes involved.

*Acknowledgements.* This work has been funded by the Swiss National Science Foundation under grant 200020-134684, MeteoSwiss in the frame of the project MIMAH, the Sodankylä LAPBIAT-2 campaign and the Oeschger Centre for Climate Research. We thank the COST Action ES604 WaVaCS. We acknowledge ECMWF for the data access of the ERA-Interim Re-



## H<sub>2</sub>O and O<sub>3</sub> anomalies during major SSW in January 2010

D. Scheiben et al.

[Title Page](#)
[Abstract](#)
[Introduction](#)
[Conclusions](#)
[References](#)
[Tables](#)
[Figures](#)




[Back](#)
[Close](#)
[Full Screen / Esc](#)
[Printer-friendly Version](#)
[Interactive Discussion](#)


AWARA): Validation and first results of the LAUTLOS/WAVVAP campaign, *J. Geophys. Res.*, 110, D13306, doi:10.1029/2004JD005543, 2005. 32396

Flury, T., Hocke, K., Haefele, A., Kämpfer, N., and Lehmann, R.: Ozone depletion, water vapor increase, and PSC generation at midlatitudes by the 2008 major stratospheric warming, *J. Geophys. Res.*, 114, D18302, doi:10.1029/2009JD011940, 2009. 32394, 32401, 32403

Forkman, P., Eriksson, P., and Winnberg, A.: The 22 GHz radio-aeronomy receiver at onsala space observatory, *J. Quant. Spectrosc. Ra.*, 77, 23–42, doi:10.1016/S0022-4073(02)00073-0, 2003. 32396

Garcia, R. R. and Solomon, S.: A new numerical model of the middle atmosphere: 2, ozone and related species, *J. Geophys. Res.*, 99, 12937–12951, 1994. 32402

Goncharenko, L. P., Coster, A. J., Chau, J. L., and Valladares, C. E.: Impact of sudden stratospheric warmings on equatorial ionization anomaly, *J. Geophys. Res.*, 115, 1–11, doi:10.1029/2010JA015400, 2010. 32394

Haefele, A., De Wachter, E., Hocke, K., Kämpfer, N., Nedoluha, G. E., Gomez, R. M., Eriksson, P., Forkman, P., Lambert, A., and Schwartz, M. J.: Validation of ground based microwave radiometers at 22 GHz for stratospheric and mesospheric water vapor, *J. Geophys. Res.*, 114, D23305, doi:10.1029/2009JD011997, 2009. 32396

Hartogh, P., Jarchow, C., Sonnemann, G. R., and Grygalashvily, M.: Ozone distribution in the middle latitude mesosphere as derived from microwave measurements at Lindau (51.66° N, 10.13° E), *J. Geophys. Res.*, 116, D04305, doi:10.1029/2010JD014393, 2011. 32394

Harvey, V. L., Randall, C. E., and Hitchman, M. H.: Breakdown of potential vorticity-based equivalent latitude as a vortex-centered coordinate in the polar winter mesosphere, *J. Geophys. Res.*, 114, 1–12, doi:10.1029/2009JD012681, 2009. 32393, 32404

Labitzke, K. and Kunze, M.: On the remarkable Arctic winter 2008/2009, *J. Geophys. Res.*, 114, D00102, doi:10.1029/2009JD012273, 2009. 32394

Lahoz, W. A., Errera, Q., Viscardy, S., and Manney, G. L.: The 2009 stratospheric major warming described from synergistic use of BASCOE water vapour analyses and MLS observations, *Atmos. Chem. Phys.*, 11, 4689–4703, doi:10.5194/acp-11-4689-2011, 2011. 32394

Lambert, A., Read, W. G., Livesey, N. J., Santee, M. L., Manney, G. L., Froidevaux, L., Wu, D. L., Schwartz, M. J., Pumphrey, H. C., Jimenez, C., Nedoluha, G. E., Cofield, R. E., Cuddy, D. T., Daffer, W. H., Drouin, B. J., Fuller, R. A., Jarnot, R. F., Knosp, B. W., Pickett, H. M., Perun, V. S., Snyder, W. V., Stek, P. C., Thurstans, R. P., Wagner, P. A., Waters, J. W., Jucks, K. W., Toon, G. C., Stachnik, R. A., Bernath, P. F., Boone, C. D., Walker, K. A., Ur-

## H<sub>2</sub>O and O<sub>3</sub> anomalies during major SSW in January 2010

D. Scheiben et al.

[Title Page](#)
[Abstract](#)
[Introduction](#)
[Conclusions](#)
[References](#)
[Tables](#)
[Figures](#)




[Back](#)
[Close](#)
[Full Screen / Esc](#)
[Printer-friendly Version](#)
[Interactive Discussion](#)


ban, J., Murtagh, D., Elkins, J. W., and Atlas, E.: Validation of the Aura Microwave Limb Sounder middle atmosphere water vapor and nitrous oxide measurements, *J. Geophys. Res.*, 112, D24S36, doi:10.1029/2007JD008724, 2007. 32397

Manney, G. L., Zurek, R. W., O'Neill, A., and Swinbank, R.: On the motion of air through the stratospheric polar vortex, *J. Atmos. Sci.*, 51, 2973–2994, 1994. 32393

Manney, G. L., Daffer, W. H., Strawbridge, K. B., Walker, K. A., Boone, C. D., Bernath, P. F., Kerzenmacher, T., Schwartz, M. J., Strong, K., Sica, R. J., Krüger, K., Pumphrey, H. C., Lambert, A., Santee, M. L., Livesey, N. J., Remsberg, E. E., Mlynczak, M. G., and Russell III, J. R.: The high Arctic in extreme winters: vortex, temperature, and MLS and ACE-FTS trace gas evolution, *Atmos. Chem. Phys.*, 8, 505–522, doi:10.5194/acp-8-505-2008, 2008a. 32394

Manney, G. L., Krüger, K., Pawson, S., Minschwaner, K., Schwartz, M. J., Daffer, W. H., Livesey, N. J., Mlynczak, M. G., Remsberg, E. E., Russell, J. M., and Waters, J. W.: The evolution of the stratopause during the 2006 major warming: Satellite data and assimilated meteorological analyses, *J. Geophys. Res.*, 113, 1–16, doi:10.1029/2007JD009097, 2008b. 32394

Manney, G. L., Schwartz, M. J., Krüger, K., Santee, M. L., Pawson, S., Lee, J. N., Daffer, W. H., Fuller, R. A., and Livesey, N. J.: Aura microwave limb sounder observations of dynamics and transport during the record-breaking 2009 Arctic stratospheric major warming, *Geophys. Res. Lett.*, 36, L12815, doi:10.1029/2009GL038586, 2009. 32394

Martius, O., Polvani, L. M., and Davies, H. C.: Blocking precursors to stratospheric sudden warming events, *Geophys. Res. Lett.*, 36, L14806, doi:10.1029/2009GL038776, 2009. 32394

Matsuno, T.: Dynamical model of stratospheric sudden warming, *J. Atmos. Sci.*, 28, 1479–1494, 1971. 32394

McInturff, R.: Stratospheric warmings: Synoptic, dynamic and general-circulation aspects, Tech. Rep. NASA-RP-1017, NASA Reference Publ., Washington, DC, 1978. 32395

Orsolini, Y. J., Urban, J., Murtagh, D. P., Lossow, S., and Limpasuvan, V.: Descent from the polar mesosphere and anomalously high stratopause observed in 8 years of water vapor and temperature satellite observations by the Odin sub-millimeter radiometer, *J. Geophys. Res.*, 115, 1–10, doi:10.1029/2009JD013501, 2010. 32394

Rodgers, C. D.: *Inverse Methods for Atmospheric Soundings*, World Scientific Publishing Co Pte. Ltd, Singapore, 2000. 32396

Rosenfield, J. E., Newman, P. A., and Schoeberl, M. R.: Computations of diabatic descent in the stratospheric polar vortex, *J. Geophys. Res.*, 99, 677–16, doi:10.1029/94JD01156, 1994.

32393

Schoeberl, M. R.: Stratospheric warmings: observations and theory, *Rev. Geophys.*, 16, 521–538, 1978. 32394

Schoeberl, M. R., Lait, L. R., Newman, P. A., and Rosenfield, J. E.: The structure of the polar vortex, *J. Geophys. Res.*, 97, 7859–7882, 1992. 32393, 32401

Seele, C. and Hartogh, P.: A case study on middle atmospheric water vapor transport during the February 1998 stratospheric warming, *Geophys. Res. Lett.*, 27, 3309–3312, 2000. 32403

Sherhag, R.: Die explosionsartigen Stratosphärenenerwärmungen des Spätwinters, 1951–1952, *Ber. Deut. Wetterdienst*, 38, 51–63, 1952. 32393

Stolarski, R. S. and Douglass, A. R.: Parameterization of the photochemistry of stratospheric ozone including catalytic loss processes, *J. Geophys. Res.*, 90, 10709–10718, 1985. 32402

Straub, C., Murk, A., and Kämpfer, N.: MIAWARA-C, a new ground based water vapor radiometer for measurement campaigns, *Atmos. Meas. Tech.*, 3, 1271–1285, doi:10.5194/amt-3-1271-2010, 2010. 32396

Waters, J. W., Froidevaux, L., Harwood, R. S., Jarnot, R. F., Pickett, H. M., Read, W. G., Siegel, P. H., Cofield, R. E., Filipiak, M. J., Flower, D. A., Holden, J. R., Lau, G. K. K., Livesey, N. J., Manney, G. L., Pumphrey, H. C., Santee, M. L., Wu, D. L., Cuddy, D. T., Lay, R. R., Loo, M. S., Perun, V. S., Schwartz, M. J., Stek, P. C., Thurstans, R. P., Boyles, M. A., Chandra, K. M., Chavez, M. C., Chen, G. S., Chudasama, B. V., Dodge, R., Fuller, R. A., Girard, M. A., Jiang, J. H., Jiang, Y. B., Knosp, B. W., LaBelle, R. C., Lam, J. C., Lee, K. A., Miller, D., Oswald, J. E., Patel, N. C., Pukala, D. M., Quintero, O., Scaff, D. M., Van Snyder, W., Tope, M. C., Wagner, P. A., and Walch, M. J.: The Earth Observing System Microwave Limb Sounder (EOS MLS) on the Aura satellite, *IEEE T. Geosci. Remote.*, 44, 1075–1092, doi:10.1109/TGRS.2006.873771, 2006. 32397

Wernli, H. and Davies, H.: A Lagrangian-based analysis of extratropical cyclones. I: The method and some applications, *Q. J. Roy. Meteorol. Soc.*, 123, 467–489, 1997. 32397

ACPD

11, 32391–32422, 2011

## H<sub>2</sub>O and O<sub>3</sub> anomalies during major SSW in January 2010

D. Scheiben et al.

Title Page

Abstract

Introduction

Conclusions

References

Tables

Figures

⏪

⏩

◀

▶

Back

Close

Full Screen / Esc

Printer-friendly Version

Interactive Discussion

## H<sub>2</sub>O and O<sub>3</sub> anomalies during major SSW in January 2010

D. Scheiben et al.

**Table 1.** Overview of the instruments and models used for the different locations. GBMW, MIAWARA, MIAWARA-C and GROMOS are ground-based microwave radiometers, MLS is the microwave limb sounder on the Aura satellite, ECMWF is the reanalysis data from the European Center for Medium-Range Weather Forecasts.

	Bern	Onsala	Sodankylä
Coordinates	46.88° N/7.47° E	57.41° N/12.02° E	67.42° N/26.6° E
H <sub>2</sub> O	MIAWARA/MLS	GBMW/MLS	MIAWARA-C/MLS
O <sub>3</sub>	GROMOS	MLS	MLS
Temperature	MLS/ECMWF	MLS/ECMWF	MLS/ECMWF
3-D Winds ( <i>u, v, w</i> )	ECMWF	ECMWF	ECMWF

Title Page

Abstract

Introduction

Conclusions

References

Tables

Figures

⏪

⏩

◀

▶

Back

Close

Full Screen / Esc

Printer-friendly Version

Interactive Discussion

## H<sub>2</sub>O and O<sub>3</sub> anomalies during major SSW in January 2010

D. Scheiben et al.

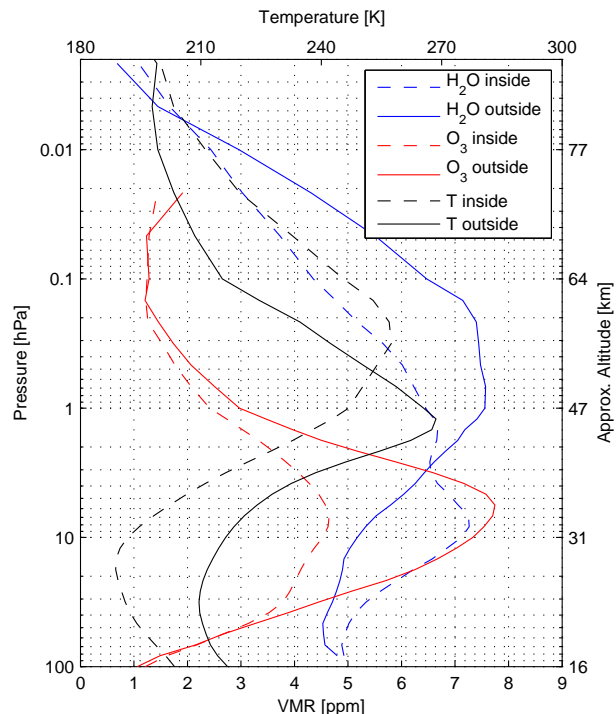


**Fig. 1.** Typical winter time profiles of middle atmospheric water vapor (blue), ozone (red) and temperature (black) for inside (dashed lines) and outside (solid lines) of the polar vortex, given in volume mixing ratio as  $\text{ppm}_v$ . The profiles and the approximate altitude are taken from Aura MLS version 3.3 for 12 January 2010, over Sodankylä (inside the vortex) and for 16 January 2010, over Bern (outside the vortex). Satellite profile selection for the two locations is within the given latitude  $\pm 400$  km and the given longitude  $\pm 800$  km. The polar vortex is determined by isentropic PV maps in the stratosphere and the location of the polar night jet in the mesosphere.

[Title Page](#)
[Abstract](#)
[Introduction](#)
[Conclusions](#)
[References](#)
[Tables](#)
[Figures](#)
[◀](#)
[▶](#)
[◀](#)
[▶](#)
[Back](#)
[Close](#)
[Full Screen / Esc](#)
[Printer-friendly Version](#)
[Interactive Discussion](#)

**H<sub>2</sub>O and O<sub>3</sub> anomalies during major SSW in January 2010**

D. Scheiben et al.

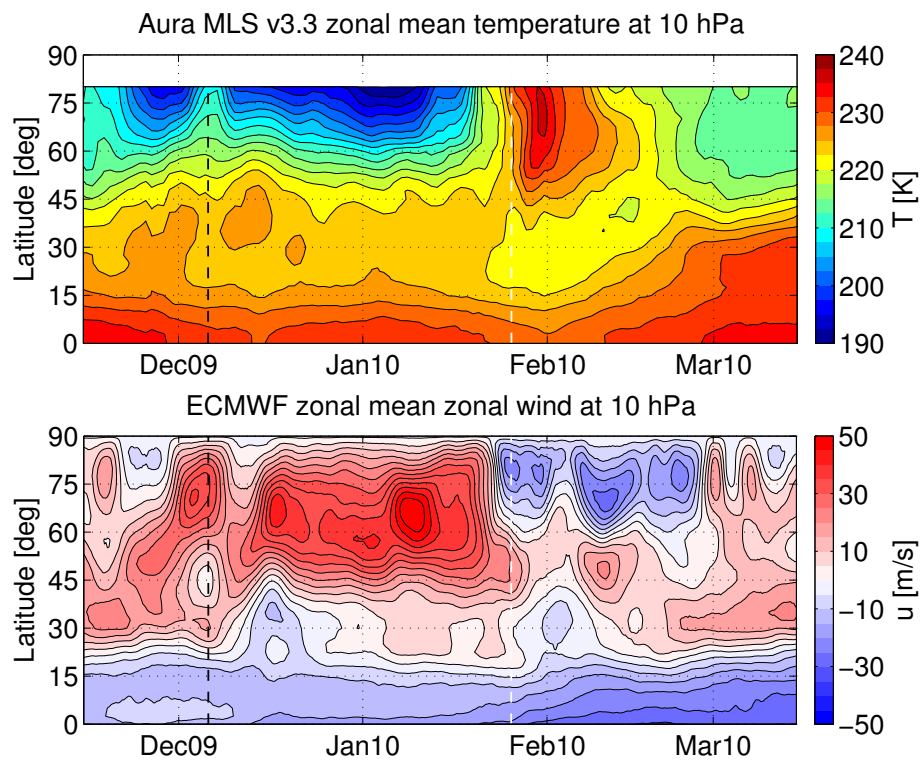


**Fig. 2.** Latitude vs. time plot of the zonal mean temperature (K) (upper panel, red (blue) colors for relatively high (low) temperatures) and zonal mean zonal wind ( $\text{m s}^{-1}$ ) (lower panel, red (blue) corresponds to eastward (westward) wind) during northern winter 2009/2010 at 10 hPa, obtained from Aura MLS and ECMWF ERA-INTERIM Re-Analysis, respectively. The vertical white dashed line indicates the start of the major SSW as defined by the WMO. The vertical black dashed line indicates the minor warming at the beginning of December 2009.

Title Page

Abstract Introduction

Conclusions References

Tables Figures

◀ ▶

◀ ▶

Back Close

Full Screen / Esc

Printer-friendly Version

Interactive Discussion



## H<sub>2</sub>O and O<sub>3</sub> anomalies during major SSW in January 2010

D. Scheiben et al.

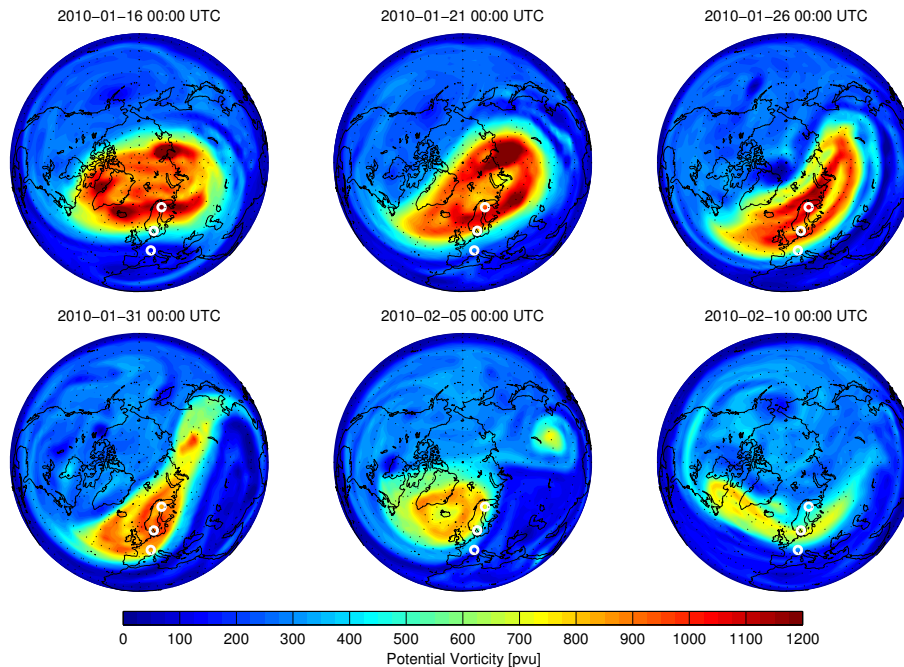


**Fig. 3.** ECMWF ERA-INTERIM Potential Vorticity (PV) maps on the 850 K isentropic surface (at approximately 10 hPa pressure level) before (16 January, upper left panel, and 21 January, upper middle panel), during (26 January, upper right panel, and 31 January, lower left panel) and after (5 February, lower middle panel, and 10 February, lower right panel) the SSW. Red (blue) colors correspond to relatively high (low) PV values. The white circles indicate the location of the microwave radiometers in Bern, Onsala and Sodankylä (from South to North).

[Title Page](#)
[Abstract](#)
[Introduction](#)
[Conclusions](#)
[References](#)
[Tables](#)
[Figures](#)
[⏪](#)
[⏩](#)
[◀](#)
[▶](#)
[Back](#)
[Close](#)
[Full Screen / Esc](#)
[Printer-friendly Version](#)
[Interactive Discussion](#)

## H<sub>2</sub>O and O<sub>3</sub> anomalies during major SSW in January 2010

D. Scheiben et al.

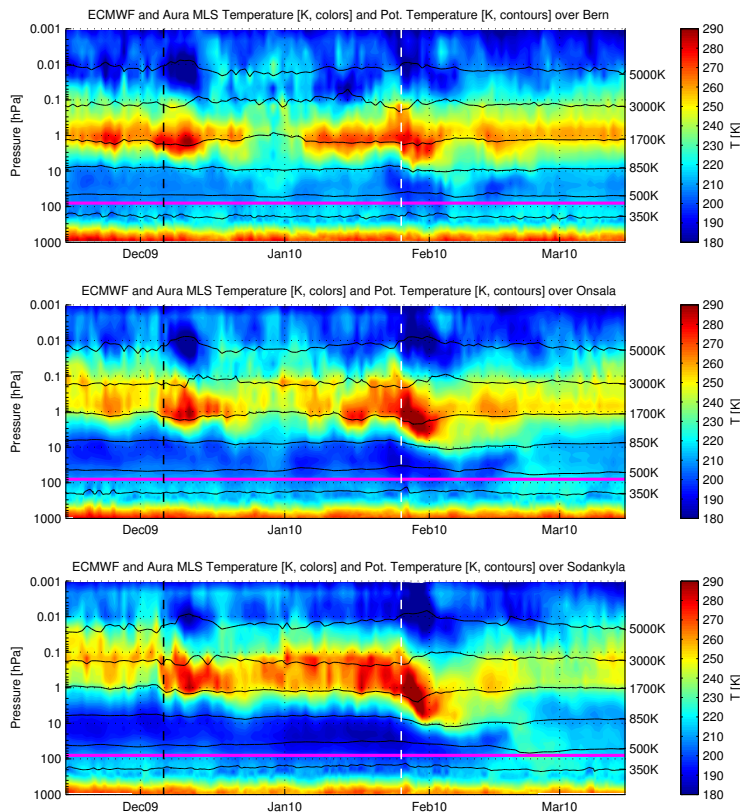


**Fig. 4.** Upper panel: Pressure vs. time plot of temperature (K) (colors) and potential temperature (K) (black contours) above Bern (47° N). Data from below 75 hPa (horizontal magenta line) is from ECMWF, above 75 hPa from Aura MLS v3.3. The vertical white dashed line indicates the beginning of the major SSW, the vertical black dashed line indicates the beginning of the minor SSW. Middle panel: For Onsala (57° N). Lower panel: For Sodankylä (67° N). Red (blue) colors correspond to relatively high (low) temperatures.

Title Page

Abstract

Introduction

Conclusions

References

Tables

Figures

◀

▶

◀

▶

Back

Close

Full Screen / Esc

Printer-friendly Version

Interactive Discussion

## H<sub>2</sub>O and O<sub>3</sub> anomalies during major SSW in January 2010

D. Scheiben et al.

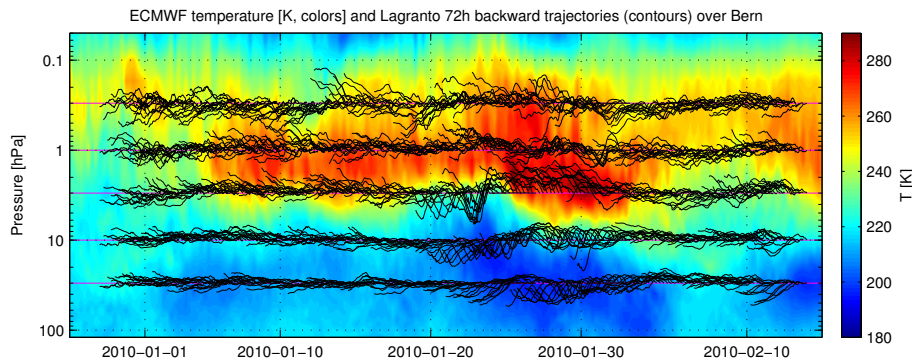


**Fig. 5.** ECMWF temperature data (K, colors) above Bern and pressure vs. time (contours) from 72 h backward trajectories, calculated with Lagranto based on ECMWF wind fields. The backward trajectories were calculated every 6 h and are ending on the magenta lines which are the selected pressure levels (0.3, 1, 3, 10 and 30 hPa) above Bern. Red (blue) colors correspond to relatively high (low) temperatures.

[Title Page](#)[Abstract](#)[Introduction](#)[Conclusions](#)[References](#)[Tables](#)[Figures](#)[◀](#)[▶](#)[◀](#)[▶](#)[Back](#)[Close](#)[Full Screen / Esc](#)[Printer-friendly Version](#)[Interactive Discussion](#)

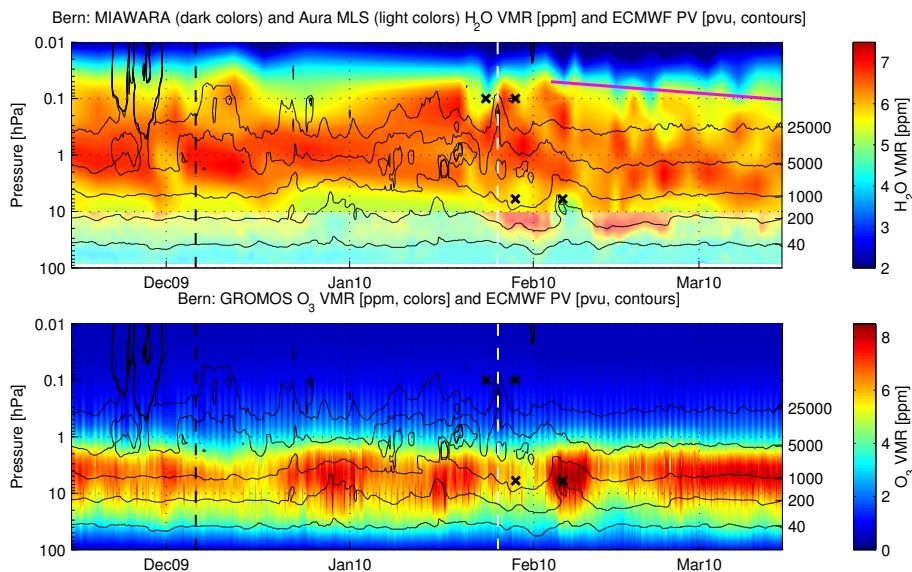


**Fig. 6.** Time series of water vapor (upper panel) and ozone (lower panel) in (ppm) over Bern. The vertical white dashed line indicates the beginning of the major SSW, the vertical black dashed line indicates the beginning of the minor SSW and the black contour lines are ECMWF PV in ( $\text{pvu} = 10^{-6} \text{K m}^2 \text{kg}^{-1} \text{s}^{-1}$ ). Red (blue) colors correspond to relatively high (low) mixing ratios. The light colors in the upper panel are Aura MLS measurements, the dark colors are ground-based microwave radiometer measurements. The black crosses are the positions from where backward trajectories were calculated. The magenta line in the upper panel indicates the subsidence of mesospheric air by using water vapor as a tracer.

## H<sub>2</sub>O and O<sub>3</sub> anomalies during major SSW in January 2010

D. Scheiben et al.

Title Page

Abstract

Introduction

Conclusions

References

Tables

Figures

◀

▶

◀

▶

Back

Close

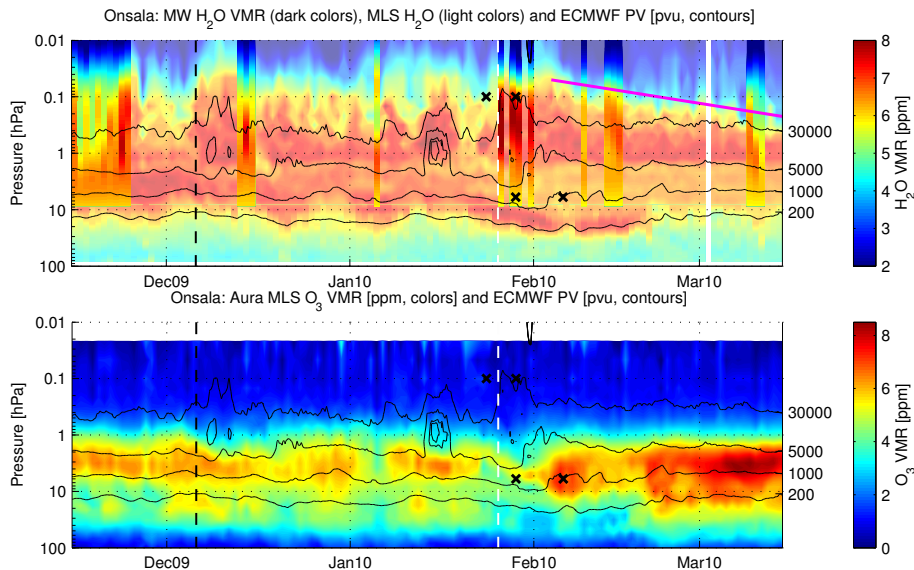
Full Screen / Esc

Printer-friendly Version

Interactive Discussion

**H<sub>2</sub>O and O<sub>3</sub> anomalies during major SSW in January 2010**

D. Scheiben et al.

**Fig. 7.** Same as Fig. 6 but for Onsala.[Title Page](#)[Abstract](#)[Introduction](#)[Conclusions](#)[References](#)[Tables](#)[Figures](#)[◀](#)[▶](#)[◀](#)[▶](#)[Back](#)[Close](#)[Full Screen / Esc](#)[Printer-friendly Version](#)[Interactive Discussion](#)

## H<sub>2</sub>O and O<sub>3</sub> anomalies during major SSW in January 2010

D. Scheiben et al.

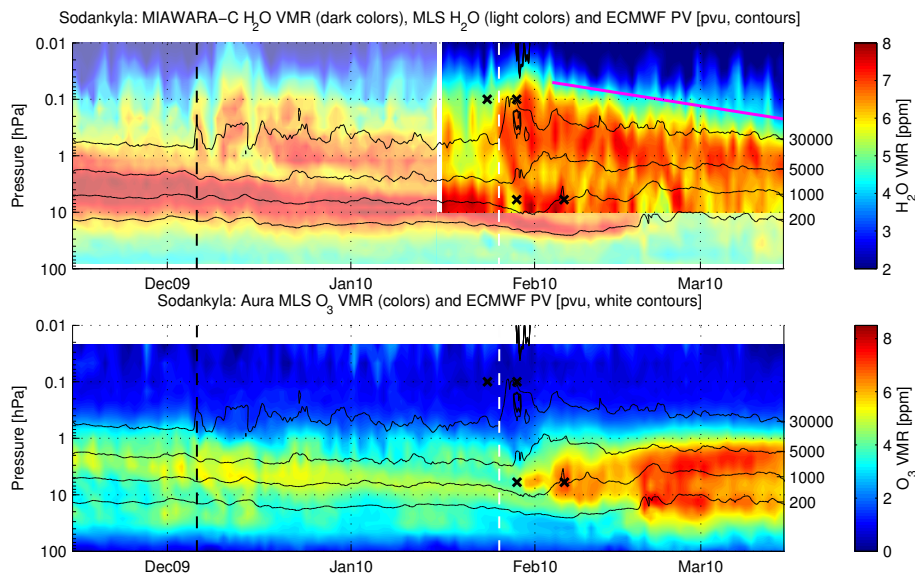
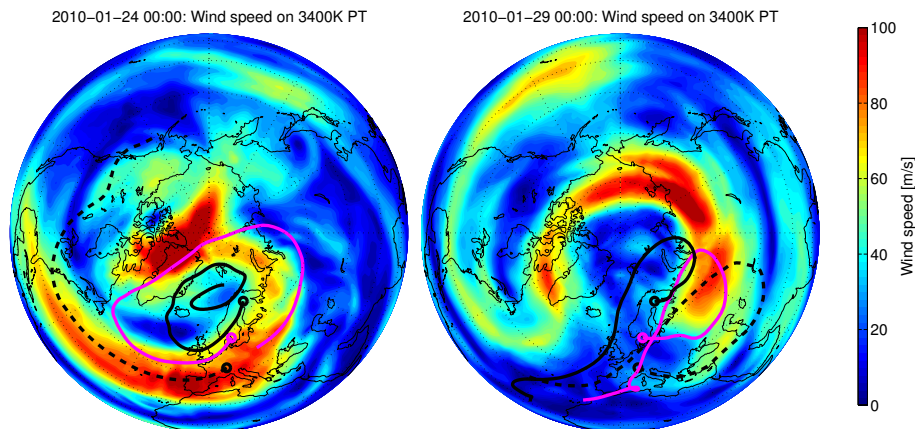


Fig. 8. Same as Fig. 6 but for Sodankylä.

[Title Page](#)[Abstract](#)[Introduction](#)[Conclusions](#)[References](#)[Tables](#)[Figures](#)[◀](#)[▶](#)[◀](#)[▶](#)[Back](#)[Close](#)[Full Screen / Esc](#)[Printer-friendly Version](#)[Interactive Discussion](#)

## H<sub>2</sub>O and O<sub>3</sub> anomalies during major SSW in January 2010

D. Scheiben et al.



**Fig. 9.** Backward trajectories (LAGRANTO, 96 h) starting from Bern (black dashed line), Onsala (magenta line) and Sodankylä (black line) superposed on polar maps of absolute wind speed (colors) ( $\text{m s}^{-1}$ ) on the 3400 K isentropic level (approximately 74 km altitude). The wind speed map in the left panel and the start of the backward trajectories are on 24 January 2010, 00:00 UTC, just before the major SSW. The wind speed map in the right panel and the start of the backward trajectories are on 28 January 2010, 00:00 UTC, just after the major SSW. Please note that the wind speed map only depicts the situation at the end of the trajectories. Red (blue) colors correspond to relatively high (low) wind speeds.

## H<sub>2</sub>O and O<sub>3</sub> anomalies during major SSW in January 2010

D. Scheiben et al.

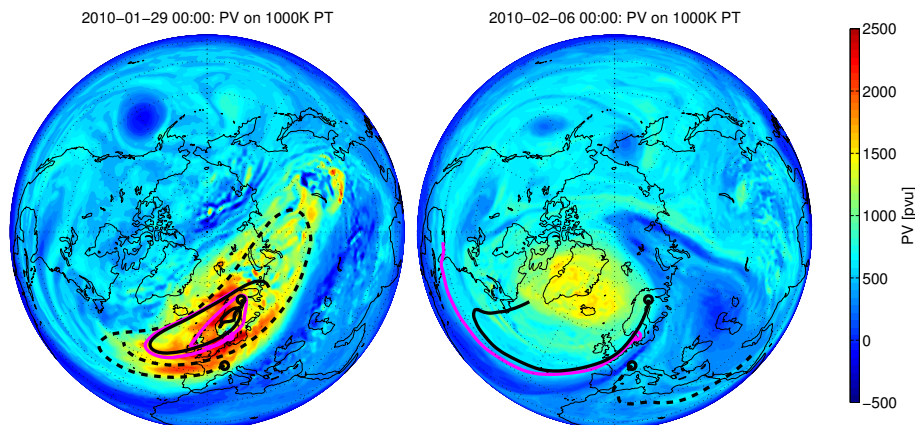


**Fig. 10.** Backward trajectories (LAGRANTO, 96 h) starting from Bern (black dashed line), Onsala (magenta line) and Sodankylä (black line) superposed on polar maps of ECMWF PV (colors) on the 1000 K isentropic level (approximately 36 km altitude). The PV map in the left panel and the start of the backward trajectories are on 28 January 2010, 00:00 UTC, just after the major SSW. The PV units shown here are  $10^{-6} \text{ Km}^2 \text{ kg}^{-1} \text{ s}^{-1}$ . The PV map in the right panel and the start of the backward trajectories are on 5 February 2010, 00:00 UTC. Please note that the PV map only depicts the situation at the end of the trajectories. Red (blue) colors correspond to relatively high (low) PV values.

[Title Page](#)[Abstract](#)[Introduction](#)[Conclusions](#)[References](#)[Tables](#)[Figures](#)[◀](#)[▶](#)[◀](#)[▶](#)[Back](#)[Close](#)[Full Screen / Esc](#)[Printer-friendly Version](#)[Interactive Discussion](#)